Journal of Hydrology 527 (2015) 978–989

Contents lists available at ScienceDirect

Journal of Hydrology

journal homepage: www.elsevier.com/locate/jhydrol

One-dimensional numerical modelling of solute transport in streams: The role of longitudinal dispersion coefficient

Kamal El Kadi Abderrezzak [a,b,*], Riadh Ata [a,b], Fabrice Zaoui [b]

[a] Saint Venant Laboratory for Hydraulics, 6 Quai Watier, 78401 Chatou, France
[b] EDF-R&D, National Laboratory for Hydraulics and Environment, 6 Quai Watier, 78401 Chatou, France

ARTICLE INFO

Article history:
Received 16 July 2014
Received in revised form 22 April 2015
Accepted 30 May 2015
Available online 5 June 2015
This manuscript was handled by Laurent Charlet, Editor-in-Chief, with the assistance of Nicolas Gratiot, Associate Editor

Keywords:
Advection–dispersion equation
Longitudinal dispersion coefficient
One-dimensional model
Solute transport

ABSTRACT

One-dimensional (1-D) numerical models of solute transport in streams rely on the advection–dispersion equation, in which the longitudinal dispersion coefficient is an unknown parameter to be calibrated. In this work we investigate the extent to which existing empirical formulations of longitudinal dispersion coefficient can be used in 1-D numerical modelling tools of solute transport under steady and unsteady flow conditions. The 1-D numerical model used here is the open source *Mascaret* tool. Its relevance is illustrated by simulating theoretical cases with known analytical solutions. Ten empirical formulas of longitudinal dispersion coefficient are then tested by simulating eight laboratory experimental cases under steady flow condition and the solute transport in the Middle Loire River (350 km long) under highly variable flow condition (from July 1st 1999 to December 31st 1999). Comparisons between computed and measured breakthrough curves show that Elder (1959), Fischer (1975) and Iwasa and Aya (1991) formulas rank as the best predictors for the experimental cases. For the field case, Seo and Cheong's (1998) formula yields the best model-data agreement, followed by Iwasa and Aya's (1991) formula. The latter formula is, therefore, recommended for the entire range of conditions studied here.

1. Introduction

The ability to predict the transport of contaminants in open channels is a major topic in many industrial and environmental projects, ranging from accidental release of pollutant to the transport of non-point sources. Solute transport is governed by a suite of hydraulic and geochemical processes, such as mixing, exchange with storage zones and biogeochemical reactions. Molecular diffusion, turbulent diffusion and shear dispersion are the fundamental mixing processes in open channels (Boxall and Guymer, 2007). Dispersion in longitudinal, lateral and vertical directions accounts for the effects of spatial differences in velocities (either primary or secondary) over the channel cross-section (Rutherford, 1994). Resolution of the equations that govern solute transport is difficult to achieve especially for field cases under unsteady flow conditions. Analytical solutions have been proposed for idealized cases, such as steady flow and instantaneous injection in prismatic open channels (De Smedt, 2006; Hunt, 2006). The application of these solutions to field cases is, however, questionable.

Numerical models have been employed in engineering studies to predict the travel time and concentration of pollutants. Several 1-D models have been proposed and every model has its advantages and limitations (Cox, 2003). The use of these models requires the hydraulic conditions are correctly simulated and the Fickian assumption is valid (*i.e.* effects of velocity shear are balanced by effects of diffusion, usually dominated by turbulent mixing) (Leibundgut et al., 2009). The development of 1-D models has focused mainly on numerical aspect of the advection–dispersion equation (Russell and Celia, 2002; Rubio et al., 2008; Shen and Phanikumar, 2009) and exchange with dead zones (Bencala and Walters, 1983; Wörman et al., 2002; Anderson and Phanikumar, 2011). Some 1-D models are limited to steady flow conditions (*e.g.* SIMCAT (UK Environment Agency, 2001), QUAL2KW (Pelletier et al., 2006), Multiphysics software COMSOL (Ani et al., 2009)), while other models simulate unsteady flows and solute transport (*e.g.* OTIS (Runkel, 1998), CCHE1D-WQ (Vieira, 2004), MIKE 11 (DHI, 2007), SD model (Deng and Jung, 2009), HEC-RAS (USACE, 2010), ADISTS (Launay et al., 2015)). Generally, validation testing has focused on theoretical cases or simplified river geometries in limited space and time scales (Zerihun et al., 2005).

* Corresponding author at: EDF-R&D, National Laboratory for Hydraulics and Environment, 6 Quai Watier, 78401 Chatou, France. Tel.: +33 130 877 911; fax: +33 130 878 109.
E-mail addresses: kamal.el-kadi-abderrezzak@edf.fr (K.E.K. Abderrezzak), riadh.ata@edf.fr (R. Ata), fabrice.zaoui@edf.fr (F. Zaoui).

http://dx.doi.org/10.1016/j.jhydrol.2015.05.061
0022-1694/

Nomenclature

A	wetted area
B	channel width
C	concentration of solute in the flow;
C^p	peak concentrations
C_l	lateral inflow solute concentration per unit length
D_L	longitudinal dispersion coefficient;
F	Froude number
$\mathbf{F}$	flux vector = $[Q, Q^2/A + gI_1]^T$
g	gravitational acceleration
H	flow depth
I_1	hydrostatic pressure force term
I_2	pressure force due to the channel walls contractions and expansions
K_s	Manning–Strickler's coefficient
Q	flow discharge
q_l	lateral flow discharge per unit length
R_e	Reynolds number
R_h	hydraulic radius
R^2	correlation coefficient
s	other point sources besides the lateral inlet solute
S	a source term of the solute = $s + C_l q_l$
$\mathbf{S}$	source term = $[q_l, gA(S_0 - S_e) + gI_2]^T$
S_e	energy slope
S_0	longitudinal bed slope
t	time
T^p	time to peak
T^0	time of starting application
$\mathbf{U}$	conservative hydraulic variables = $[A, Q]^T$
V	flow velocity
V_*	shear velocity
x	longitudinal coordinate
y	lateral coordinate
z	vertical coordinate
z_b	bed elevation
ΔC^p	mean relative error of concentration
ΔC^p	mean relative error of peak concentration
Δt	time step
ΔT^p	mean relative error of phase
Δx	space step
ρ	density of water
ε_t	transverse mixing coefficient

All 1-D solute transport models rely on the advection–dispersion equation, which brings the longitudinal dispersion coefficient, D_L, as unknown parameter to be determined. This coefficient measures the intensity of longitudinal dispersion, which is the primary mechanism that is responsible for reducing peak concentrations once the cross-sectional mixing is complete (Chen et al., 2009). In most numerical models, D_L is assumed to be time and space invariant, and estimated with field tracer experiments, with values varying within a range of 10^{-1}–10^7 m^2/s (Seo and Cheong, 1998). Field tracer studies can be expensive and time-consuming, especially for large rivers (Shen et al., 2010; Kim, 2012), and the dispersion coefficient estimate is valid for only the stream reach examined and the set of hydraulic conditions during which the tracer experiment was conducted. Therefore, water quality modellers often use semi-analytical and empirical formulations, relating D_L to flow and channel properties. Most formulas were derived from different assumptions and tested using laboratory and field data sets, and when applied to one study case the estimated dispersion coefficients for the different formulas may vary over several orders of magnitude (Rutherford, 1994). Performance of formulations has been usually assessed by comparing calculated and measured dispersion coefficients (Tayfur and Singh, 2005; Sahay, 2011; Etemad-Shahidi and Taghipour, 2012; Zeng and Huai, 2014), with the measured values being deduced from the observed transverse velocity profiles using the volume integral expression (Deng et al., 2001; Seo and Baek, 2004) or from the temporal concentration profiles using statistical approaches such as moments method (Ho et al., 2002; Zhang et al., 2006) and Chatwin method (Chatwin, 1980). Only some authors investigated the accuracy of selected formulas by comparing numerically calculated breakthrough curves with measurements (Kashefipour and Falconer, 2002; Ani et al., 2009). However, they solved the advection–dispersion equation assuming averaged flow variables in the river, which requires the flow to be steady and the bed geometry to be prismatic. The application of longitudinal dispersion coefficient formulas to geometrically non-uniform channels and unsteady flow conditions is therefore still needed.

In this work we make a step forward and investigate the suitability of dispersion coefficient formulas in 1-D modelling of solute transport under steady and unsteady flow conditions. In contrast to many works published in the literature, the performance of each formula is assessed in the current paper by comparing the calculated breakthrough curves of concentration with measurements. We restrict our attention to non-reactive solutes. We use the Mascaret code, which is the 1-D component of the open source Telemac-Mascaret system developed at EDF-R&D (www.opentelemac.org The code incorporates dispersion coefficient formulas proposed by Elder (1959) (noted hereafter E), Fischer (1975) (F), McQuivey and Keefer (1974) (M&K), Liu (1977) (L), Iwasa and Aya (1991) (I&A), Magazine et al. (1988) (M), Koussis and Rodriguez-Mirasol (1998) (K&R-M), Seo and Cheong (1998) (S&C), Deng et al. (2001) (D) and Kashefipour and Falconer (2002) (K&F).

The remainder of the paper is set out as follows: Section 2 presents the modelling framework. A brief background to the investigated dispersion coefficient formulas is provided in Section 3. In Section 4, the performance of the formulas is assessed using eight laboratory experimental cases under steady flow. In Section 5, formulas are applied for simulating solute transport along the 350 km of the Loire River (France) over the period July 1st 1999 to December 31th 1999. A discussion is given in Section 6, followed by conclusions in Section 7.

2. Formulation of the problem and numerical scheme

The description of the modelling tool given herein is brief. *Mascaret* has been extensively applied for simulating flow propagation in open channels, through the framework of the EU-project CADAM (Goutal, 1999), and solute transport through the IAEA-project EMRAS (Goutal et al., 2008). However, the pure advection term of the solute transport equation was solved by the method of characteristics. In all numerical runs (*i.e.* experimental and field cases), we use a second order finite volume scheme (FV2). Its relevance is demonstrated hereafter using two theoretical cases.

2.1. Basic equations for flow

Based on the hydrostatic pressure distribution and incompressible flow assumptions, the flow hydrodynamics is represented by

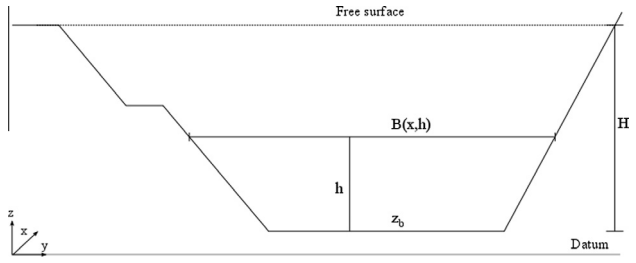

Fig. 1. Definition diagram for the numerical model.

the 1-D shallow water equations. Defining a Cartesian coordinate system (x,y,z), with the x-axis longitudinal, y-axis transversal and the z-axis vertical upward (Fig. 1), the system of equations is expressed in the conservative form as

$$\frac{\partial \mathbf{U}}{\partial t} + \frac{\partial \mathbf{F}(\mathbf{U})}{\partial x} = \mathbf{S}(x, \mathbf{U}) \tag{1}$$

where t is time, $\mathbf{U} = [A, Q]^T$ is the conserved variables, $\mathbf{F}(\mathbf{U}) = [Q, Q^2/A + gI_1]^T$ is flux, $\mathbf{S}(x, \mathbf{U}) = [q_l, gA(S_0 - S_e) + gI_2]^T$ is source terms, A is the wetted area, Q is the flow rate, q_l is the lateral flow rate per unit length, g is the gravitational acceleration, $S_0 = -z_b/x$ is the longitudinal bed slope with z_b as the bed level, $S_e = QQ/(K_s^2 A^2 R_h^{4/3})$ is the energy slope computed using Manning–Strickler's equation (with R_h as the hydraulic radius and K_s as Manning–Stricker's coefficient), I_1 is the hydrostatic pressure force term (Eq. (2a)) and I_2 represents a pressure force term that accounts for the forces exerted by the channel contraction and expansion (Eq. (2b)).

$$I_1 = \int_0^H (H - h) B(x, h) dh \tag{2a}$$

$$I_2 = \int_0^H (H - h) \frac{\partial B(x, h)}{\partial x} dh \tag{2b}$$

where H is the flow depth, B is the width, and h is the vertical distance above the bottom.

2.2. Advection–dispersion equation

The transport equation for a constituent is described by the advection–dispersion equation

$$\frac{\partial AC}{\partial t} + \frac{\partial (QC)}{\partial x} = \frac{\partial}{\partial x}\left(D_L A \frac{\partial C}{\partial x}\right) + C_l q_l \tag{3}$$

where C is the solute concentration in the flow, and C_l is the lateral inflow solute concentration per unit length of channel. The dispersion coefficient D_L is prescribed by an empirical formulas (see Section 3).

2.3. Numerical scheme

The flow and advection–dispersion equations are solved sequentially in decoupled way. First, the flow module provides the time-dependent hydraulic variables throughout the domain, and then these variables are passed to the water quality module for the solute transport simulation. For steady flows, Eq. (1) is solved using a finite difference scheme. For transient mixed flows, a first-order Godunov-type explicit scheme is employed (Goutal and Maurel, 2002).

The advection and dispersion terms of Eq. (3) are computed within a fractional step algorithm. The advection term is solved by a second order finite volume scheme (FV2), which is of higher accuracy compared to finite difference and finite element methods of the same order (Zhang and Aral, 2004). Indeed finite volume schemes are the most suitable approach for advection dominated processes, while they are locally conservative (among other advantages). A Superbee limiter function suppresses numerical oscillations, while still maintaining a first order resolution at discontinuities and higher order accuracy in the smooth regions. In the second step, an implicit scheme is applied to the dispersion equation.

Because the numerical scheme is explicit in flow and pure advection computations, the time step should be limited by stability conditions. The Courant–Friedrichs–Levy (CFL) condition for flow is used, with the Courant number being limited to 1.0 in the present study. For the solute concentration, a Dirichlet condition is used at the upstream boundary and a Neumann condition is imposed at the downstream end.

2.4. Evaluation of the advective step in numerical solution

The accuracy of the numerical scheme for the advection step is evaluated using two theoretical tests with steep concentration gradients: rectangular and sinusoidal profiles. These profiles are selected because they represent the highest degree of difficulty to the numerical solution of the advection equation (Zoppou et al., 2000). The flume is horizontal, rectangular, 1.00 m width, 1.00 m deep and 2000 m length. The flow is uniform, $Q = 0.5\ m^3\ s^{-1}$ and $H = 0.50$ m. The solute is injected at the upstream end of the channel, begins 30 min after the start of water flowing and ends 10 min later. The space step Δx is 5 m and the time step Δt is 2.5 s. Because dispersion is not considered, the inlet concentration profile is expected to move in the downstream direction at uniform velocity.

Fig. 2 plots the longitudinal profile of solute concentration at various times. The numerical results obtained by the second order finite volume scheme (FV2) are free of oscillations and the general

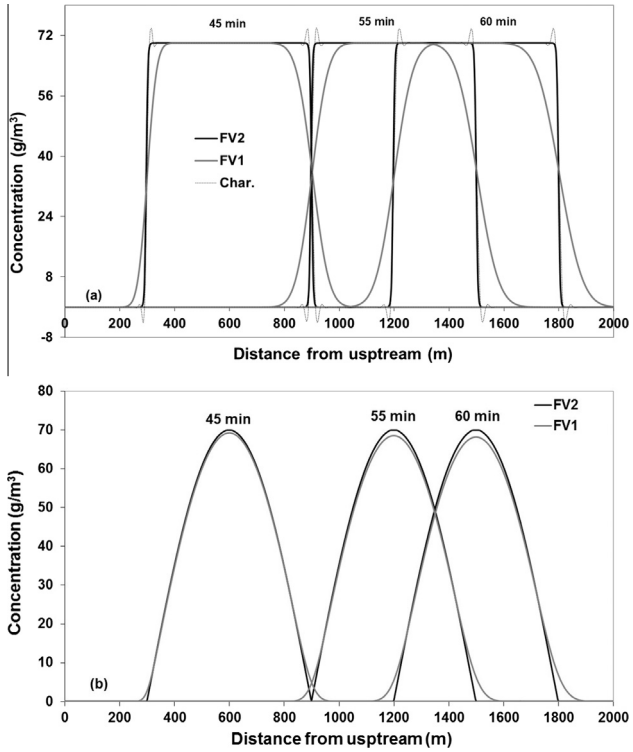

Fig. 2. Advection of concentration profiles along the channel at three time steps. (a) Trapezoidal profile and (b) sinusoidal profile (Char. and FV2 provide equivalent results).

shape (magnitude and variance) of the concentration profiles remains unchanged. Using the first order finite volume scheme (FV1), the concentration profile progressively shrinks as it moves downstream, mainly due to numerical diffusion. The method of characteristics (Char.), applied to the conservative form of the advection equation, generates oscillations (Fig. 2) in the case of rectangular profile concentration, but performs very well for the sinusoidal shape (*i.e.* similar results as those of FV2). Both cases confirm that FV2 scheme is more efficient than FV1 and Char. methods.

2.5. Comparison of analytical and numerical solutions

Here we simulate solute transport in the same channel as that described previously. The flow is uniform, the solute inlet injection is constant and the dispersion coefficient D_L is time and space invariant. The following analytical solution was proposed by Warrick (2003)

$$C(x,t) = C_i + 0.5(C_0 - C_i)\left[erfc\left(\frac{x - V(t-t_0)}{2\sqrt{D_L(t-t_0)}}\right) + \exp\left(\frac{Vx}{D_L}\right) erfc\left(\frac{x + V(t-t_0)}{2\sqrt{D_L(t-t_0)}}\right)\right] \quad (4)$$

where C_0 is the concentration at the channel inlet, C_i is the initial concentration, and t_0 = time (measured from the beginning of the simulation) at which solute injection begins and V is the flow velocity. In the present run, $Q = 1\ m^3\ s^{-1}$, $H = 0.5$ m, $C_0 = 70\ g\ m^{-3}$ injected at 10 min until inflow cut-off at 60 min, C_i is set at zero, $D_L = 10\ m\ s^{-1}$, $\Delta x = 25$ m and $\Delta t = 30$ s. The FV2 scheme is used. The breakthrough curves obtained by the numerical and analytical models are shown in Fig. 3. Again, numerical results are free of oscillations and match closely the analytical solution.

3. Review of longitudinal dispersion coefficient formulas

Considerable uncertainty exists about the prescription of the dispersion coefficient D_L, because D_L is closely related to the hydraulics variables, characteristics of the fluid (*e.g.* viscosity), the sediment transport (*e.g.* suspension) and channel geometry (*e.g.* cross-sectional shape, planform curvature) (Toprak et al., 2004). In this paper, we examine the skill of ten formulas proposed by Elder (1959) ("E"), Fischer (1975) ("F"), McQuivey and Keefer (1974) ("M&K"), Liu (1977) ("L"), Iwasa and Aya (1991) ("I&A"), Magazine et al. (1988) ("M"), Koussis and Rodriguez-Mirasol (1998) ("K&R-M"), Seo and Cheong (1998) ("S&C"), Deng et al. (2001) ("D") and Kashefipour and Falconer (2002) ("K&F"). Table 1 contains the formulations and summarises the conditions for their calibration and validation.

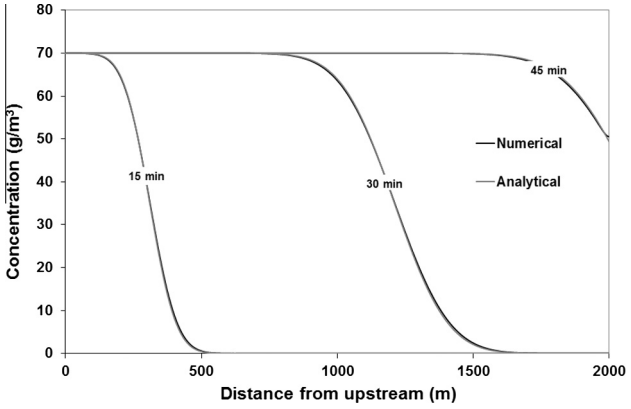

Fig. 3. Comparison of analytical and numerical solutions of advection–diffusion using FV2. Solute concentration along the channel at three times.

All formulas are related to cross-sectional mean parameters, which are obtained from 1-D numerical models. Calibration and validation of the formulas have been performed using dispersion coefficient data derived from laboratory and field tracer studies. Elder's equation includes only vertical variations in the mean velocity, and the velocity distribution is assumed to be logarithmic. This was criticized by many authors (Seo and Baek, 2004), arguing that the transverse profile of the velocity is far more important in producing the longitudinal dispersion than is the vertical profile. Using transverse instead of vertical velocity variations, many predictive formulas have been proposed in the following form in which B/H and V/V_* account for transverse velocity gradient effect and turbulent shear intensity, respectively.

$$\frac{D_L}{HV_*} = \alpha\left(\frac{V}{V_*}\right)^{\beta}\left(\frac{B}{H}\right)^{\lambda} \quad (5)$$

where V_* is the shear velocity and α, β and λ are coefficients. For rivers under nearly uniform flow conditions, all formulas indicate that D_L remains space invariant. This was contested experimentally (Singh et al., 1992). Recently, Launay et al. (2015) reviewed some empirical dispersion formulas. Variability of $D_L/(HV_*)$ with B/H and V/V_*, respectively, was analysed using laboratory and field data sets. They found that laboratory data follows the same trend as field data according to B/H. However, the laboratory data corresponding to narrow flumes ($B/H < 30$) yields lower D_L values compared to field cases with similar V/V_* values. Launay et al. (2015) argued that the formulas for which the fit was mainly based on B/H (*e.g.* "L", "I&A", "K&R-M") are generally more appropriate for field data. On the contrary, formulas with a large β-value (*e.g.* "F", "S&C", "D") are too sensitive to the calculation of V/V_*, which often induces larger uncertainties in field data.

4. Transport of tracer (Rhodamine WT) in laboratory flumes

In this section we simulate eight experimental laboratory cases conducted by Zulfequar (1997) at the Civil Engineering Department of the University of Roorkee (India). The experiments covered a laboratory program wherein longitudinal dispersion of conservative pollutant was investigated under uniform flow conditions.

4.1. Overview of the experiments

The flume is rectangular, 0.20 m width, 0.50 m deep and 30 m length. The flow was maintained uniform by adjusting a tailgate at the downstream end of the flume. Rhodamine WT was injected near the upstream end of the flume. Concentrations were monitored at four locations using a Turner Fluorometer. Experiments were conducted for three values of bed slope and various inflow discharges (Table 2), under subcritical (Froude number F smaller than 0.9) and turbulent (Reynolds number R_e larger than 10^4) conditions. The width-depth ratio B/H ranged between 1.5 and 3 and the roughness ratio V/V_* was in the range 17–18.5.

Zulfequar (1997) showed that mixing took place at the first location (4–5 m downstream of the injection). Therefore, the measured concentration curve on the first station is used as Dirichlet condition in the numerical runs; computed and measured concentrations are compared at the remaining three locations. The Manning–Strickler coefficient for each run is calibrated using the flow depth, discharge and longitudinal bed slope (*i.e.* uniform flow condition) (Table 2). In the numerical runs, $\Delta t = 0.005$ s and $\Delta x = 0.01$ m. It is worth noting that the tracer mass balance was checked for each numerical run by comparing the mass which is

Table 1
Review of selected longitudinal dispersion formulas.

Reference	Formula	Comments/conditions for formula calibration and verification
Elder (1959) (E)	$D_L = 5.93HV_*$	Uniform flow in an infinitely wide channel Logarithmic vertical-velocity distributions Mixing coefficients for momentum and mass transfer are assumed identical
Fischer (1975) (F)	$D_L = 0.011\left(\frac{V}{V_*}\right)^2\left(\frac{B}{H}\right)^2 hV_*$	Validated using measurements in straight prismatic channels of various regular cross-sectional shapes
McQuivey and Keefer (1974) (M&K)	$D_L = 0.058\frac{HV}{S_e}$	Developed using the similarity between 1-D solute dispersion equation and 1-D flow propagation equation Regression of field data from 18 rivers to find constant of proportionality Flow regime with Froude number smaller than 0.5
Liu (1977) (L)	$D_L = 0.18\left(\frac{V}{V_*}\right)^{0.05}\left(\frac{B}{H}\right)^2 HV_*$	Obtained using Fischer's equation and incorporating the role of lateral velocity gradient The term $0.18(V/V_*)^2$ relates to the cross-sectional geometry and to the transverse velocity distributions Calibrated and validated using field data from 14 rivers
Iwasa and Aya (1991) (I&A)	$D_L = 2HV_*\left(\frac{B}{H}\right)^{1.5}$	Calibrated using 62 laboratory experiments in small scale flumes and field data sets from 79 rivers
Magazine et al. (1988) (M)	$D_L = 75.86\left(0.4\frac{V}{V_*}\right)^{-1.632}R_hV$	Developed using dimensional analysis and calibrated on the basis of laboratory experimental data sets
Koussis and Rodriguez-Mirasol (1998) (K&R-M)	$D_L = 0.6HV_*\left(\frac{B}{H}\right)^2$	Based on the original theory and equation proposed by Fischer and von Karman's defect law The value of 0.6 was found by applying a regression analysis on field data from 16 rivers ($B/H > 6$)
Seo and Cheong (1998) (S&C)	$D_L = 5.92\left(\frac{V}{V_*}\right)^{1.43}\left(\frac{B}{H}\right)^{0.62}HV_*$	Developed using dimensional analysis and the one-step Huber method Calibrated and validated using data sets from 26 streams in USA
Deng et al. (2001) (D)	$D_L = \frac{0.15}{8\varepsilon_t}\left(\frac{V}{V_*}\right)^2\left(\frac{B}{H}\right)^{1.67}HV_*$ with $\varepsilon_t = 0.145 + (V/V_*)(B/H)^{1.38}/3520$	This formula is a revised version of Fischer's equation, integrating a new expression of the transverse mixing coefficient ε_t and the influence of transient storage zones Calibrated and validated using field data from 29 rivers ($B/H > 10$)
Kashefipour and Falconer (2002) (K&F)	$D_L = 10.612\left(\frac{V}{V_*}\right)HV$ for $B/H > 50$ $D_L = \left[7.428 + 1.775\left(\frac{B}{H}\right)^{0.62}\left(\frac{V_*}{V}\right)^{0.572}\right]\left(\frac{V}{V_*}\right)hV$ for $B/H < 50$	Developed using dimensional and regression analysis Calibrated and validated using data sets from 30 streams in USA

Table 2
Flow parameters in Zulfequar's experiments.

Exp.	S_0	Q ($m^3\ s^{-1}$)	H (m)	V ($m\ s^{-1}$)	K_s ($m^{-1/3}\ s^{-1}$)	F	R_e
Zul1	0.004546	0.01053	0.0700	0.7521	93.55	0.90	24×10^4
Zul2	0.004546	0.02188	0.1200	0.9117	94.01	0.84	38×10^4
Zul3	0.004546	0.01863	0.1118	0.8332	87.82	0.80	34×10^4
Zul4	0.002470	0.01053	0.0915	0.5754	87.93	0.61	21×10^4
Zul5	0.002470	0.01558	0.1243	0.6267	86.75	0.57	27×10^4
Zul6	0.001488	0.01317	0.1309	0.5031	88.38	0.44	22×10^4
Zul7	0.001488	0.01442	0.1388	0.5195	89.75	0.44	23×10^4
Zul8	0.001488	0.00833	0.0900	0.4628	91.64	0.50	17×10^4

present in the channel at the end of the simulation (the tracer does not reach the downstream end) with that injected at the upstream end. The total mass was accurately maintained within an accuracy of 99.4%.

4.2. Results and comparison

For the sake of brevity, we show the results obtained using the two formulas that give the best and worst results, respectively. The experimental dispersion coefficient was estimated for each case using the moment method, which is suitable for uniform flow conditions (Zhang et al., 2006). Values are summarized and compared with those computed empirically in Table 3. The "M&K", "S&C", "D" and "K&F" equations overestimate significantly the value of D_L, then followed by "M" formula. The best results are obtained with "E", "F", "I&A", "L", "K&R-M" equations. Fig. 4 reports the measured and computed breakthrough curves. Table 4 summarizes the mean relative errors. The performance of one formula depends on the conditions of the experiment. The "E" formula yields the best agreement between the simulated and observed concentrations for Zul3 and Zul7 cases with ΔC^p and ΔT^p smaller than 5%, followed by "F" and "I&A" formulas. "F" formula provides better results for Zul2, Zul5 and Zul8 experiments (*i.e.* ΔC^p and $\Delta T^p < 8\%$) followed by "E" and "I&A" formulas. "I&A" formula is preferable when simulating Zul1, Zul4 and Zul6 experiments (*i.e.* ΔC^p and $\Delta T^p < 6.5\%$), followed by "E", "F" and "L" formulas.

Analysis of the best formulas (*i.e.* "E", "F", "I&A", "L") reveals that the computed peak times are shifted compared to observations, although the relative error can be judged acceptable (5% on average, Table 4). Reasons for such shifting may include (i) measurement uncertainties, (ii) experimental conditions which do not guarantee well-established uniform regime, (iii) non constant dispersion coefficient even for such simple configuration, and (vi) numerical accuracy of the flux estimation.

The threshold of error below which the performance of one formula is judged acceptable is subjective. For field cases, Kashefipour and Falconer (2002) considered the computed concentrations as accurate when the mean relative error was lower than 35%. In this work, we can claim that a formula giving relative errors smaller than 15% is working well, because the simulated experimental cases are simple. On this ground, "E", "F" and "I&A" formulas rank as the best predictors for the entire range of experimental conditions (Table 3), with ΔC^p and ΔT^p being smaller than 14% and 7%, respectively. Moreover, ignoring the discrepancy in the tracer arrival time, the three formulas properly reproduce the tail and falling limb of the measured breakthrough curves, with determination coefficients larger than 0.87.

Regarding the formulas that provide less satisfactory results at least for one experiment, "M&K", "S&C", "D" and "K&F" equations underestimate concentrations systematically, yielding ΔC^p in the range of 40–62%: the largest errors are obtained by the "S&C" formulation, which overpredicts significantly the arrival time of the tracer. The computed arrival time of the peak concentration obtained by "M&K" and "D" formulas is, however, in good agreement with measurements; less satisfactory results are provided

Table 3
Zulfequar's experiments – Measured and computed dispersion coefficients.

Exp.	Mesasured (m^2/s)	Computed (m^2/s)									
		E	F	M&K	L	I&A	M	K&R-M	S&C	D	K&F
Zul1	3.7×10^{-2}	1.7×10^{-2}	6.3×10^{-2}	67×10^{-2}	2×10^{-2}	2.9×10^{-2}	10×10^{-2}	1.4×10^{-2}	204×10^{-2}	60×10^{-2}	747×10^{-2}
Zul2	5.6×10^{-2}	3.5×10^{-2}	6.2×10^{-2}	140×10^{-2}	1.3×10^{-2}	2.6×10^{-2}	14×10^{-2}	0.9×10^{-2}	311×10^{-2}	57×10^{-2}	1595×10^{-2}
Zul3	5.0×10^{-2}	3.2×10^{-2}	5.6×10^{-2}	118×10^{-2}	1.2×10^{-2}	2.5×10^{-2}	13×10^{-2}	1.1×10^{-2}	268×10^{-2}	50×10^{-2}	1268×10^{-2}
Zul4	3.7×10^{-2}	1.8×10^{-2}	4.7×10^{-2}	123×10^{-2}	1.1×10^{-2}	2.0×10^{-2}	9×10^{-2}	0.9×10^{-2}	171×10^{-2}	39×10^{-2}	712×10^{-2}
Zul5	5.1×10^{-2}	2.7×10^{-2}	3.8×10^{-2}	183×10^{-2}	0.8×10^{-2}	1.8×10^{-2}	11×10^{-2}	0.7×10^{-2}	210×10^{-2}	36×10^{-2}	1052×10^{-2}
Zul6	2.7×10^{-2}	2.2×10^{-2}	2.9×10^{-2}	256×10^{-2}	0.7×10^{-2}	1.4×10^{-2}	9×10^{-2}	0.5×10^{-2}	173×10^{-2}	28×10^{-2}	907×10^{-2}
Zul7	2.6×10^{-2}	2.4×10^{-2}	3.9×10^{-2}	162×10^{-2}	0.9×10^{-2}	1.6×10^{-2}	7×10^{-2}	0.7×10^{-2}	138×10^{-2}	32×10^{-2}	586×10^{-2}
Zul8	2.2×10^{-2}	1.4×10^{-2}	2.9×10^{-2}	281×10^{-2}	0.6×10^{-2}	1.4×10^{-2}	9×10^{-2}	0.5×10^{-2}	185×10^{-2}	29×10^{-2}	1010×10^{-2}

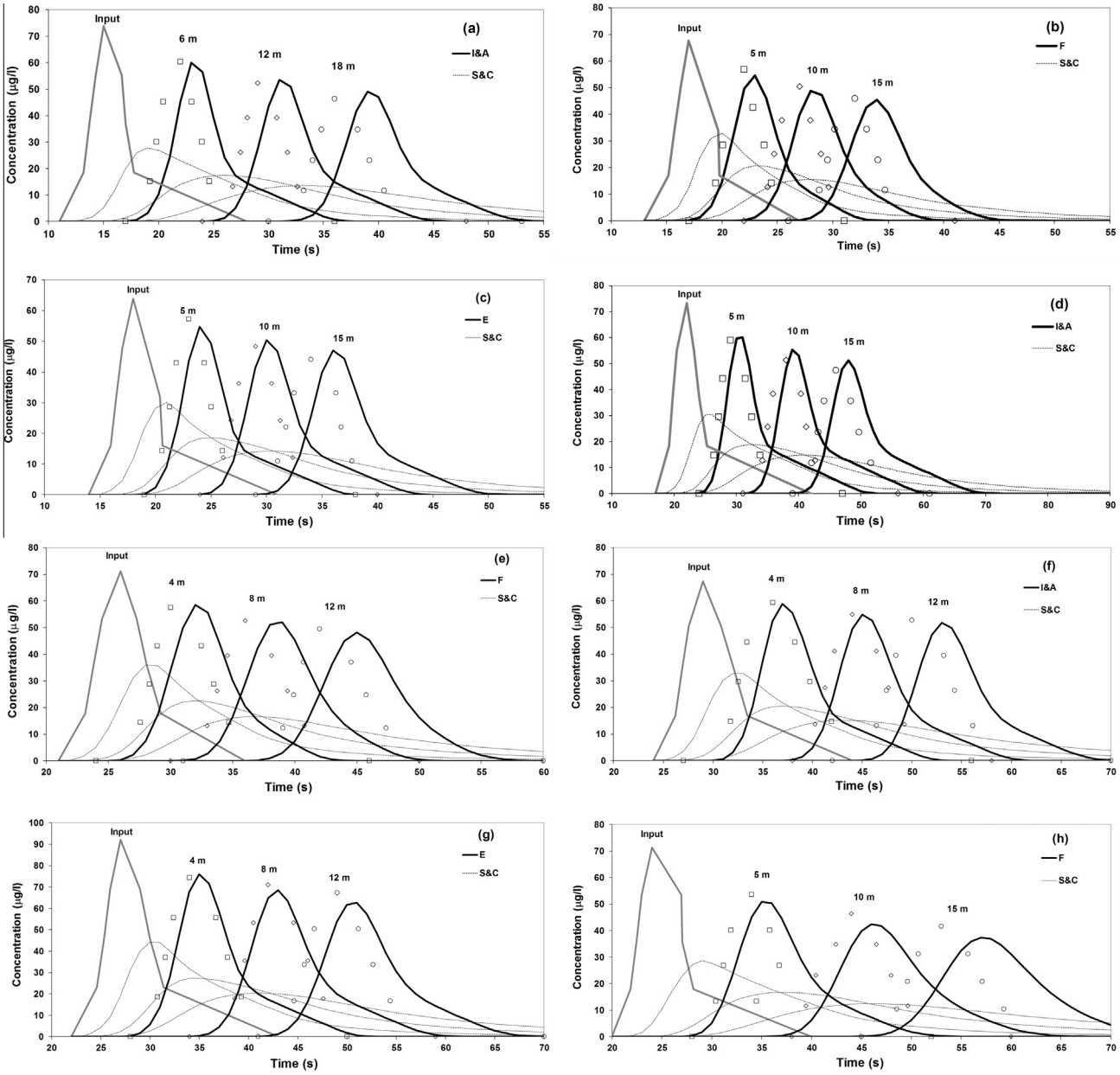

Fig. 4. Zulfequar's (1997) experiments. Comparison between computed and measured concentrations at three locations. Symbols = measurements, lines = numerical results. (a) Zul1; (b) Zul2; (c) Zul3; (d) Zul4; (e) Zul5; (f) Zul6; (g) Zul7; and (h) Zul8.

Table 4
Zulfequar's experiments. Summary of accuracy of the formulas.

	Relative Error (%)	E	F	M&K	L	I&A	M	K&R-M	S&C	D	K&F
Zul1	ΔC^p[a]	11	12	56	13	**3**	23	16	64	54	60
	ΔT^p[b]	6	6	4	6	**6**	6	6	12	2	28
Zul2	ΔC^p	6	**3**	53	16	10	18	18	56	43	51
	ΔT^p	5	**4**	4	5	5	5	5	12	1	26
Zul3	ΔC^p	**5**	7	56	13	7	25	15	59	52	51
	ΔT^p	**5**	5	3	5	5	5	5	11	1	24
Zul4	ΔC^p	7	10	60	16	**6**	25	18	60	50	52
	ΔT^p	5	3	9	5	**5**	4	5	11	1	28
Zul5	ΔC^p	5	**2**	53	18	10	22	20	54	42	40
	ΔT^p	7	**7**	8	7	7	6	7	11	4	21
Zul6	ΔC^p	7	8	58	7	**1**	29	11	60	50	46
	ΔT^p	4	4	17	4	**4**	4	4	14	2	25
Zul7	ΔC^p	**4**	6	57	14	5	28	18	57	47	42
	ΔT^p	**3**	3	9	5	3	2	3	16	1	26
Zul8	ΔC^p	14	**8**	58	23	11	21	30	60	51	50
	ΔT^p	6	**5**	19	5	6	4	5	14	2	30

[a] Mean relative error of peak $\Delta C^p[\%] = 100 \times \sum_{i=1}^{N} |(C^p_{c,i} - C^p_{m,i})/C^p_{m,i}/N$.
[b] Mean relative error of phase $\Delta T^p[\%] = 100 \times \sum_{i=1}^{N} |(T^p_{c,i} - T^p_{m,i})/(C^p_{m,i} - T^0)/N$. C^p_c and C^p_m are the computed and measured peak concentrations, respectively; T^p_c and T^p_m the computed and measured times to peak, respectively; T^0 time of starting application, the subscript i refers to the station where concentration is monitored, N the total number of stations (=3). In bold: best match between measurements and numerical results.

by "S&C" and "K&F". Correspondence between observed and simulated concentrations is improved using the "L", "K&R-M" and "M" formulas but deviations are still not negligible (*i.e.* ΔC^p in the range of 6–29%).

5. Transport of tritium in the Middle Loire River

In this section we examine the performance of the dispersion coefficient formulas by simulating the transport of tritium in the Middle Loire River (France) under unsteady flow conditions during the period 07/01/1999–12/31/1999.

The Loire River is the longest river in France with a length of 1012 km. Its drainage area represents 117,000 km^2, that is one fifth of France's area. The reach studied is the Middle Loire, 350 km long extending from Belleville (Pk532.82) to MontJean (Pk885.37) (with Pk denotes the distance in km measured along the river course from its source), with a catchment area of 109,930 km^2 (Fig. 5). This reach has an average width and slope of about 400 m and 0.0004, respectively. Four tributary streams feed the river: Vienne, Indre and Cher on the left side and Maine on the right side. The hydrologic regime is highly variable (*i.e.* pluvio-nival regime of the Mediterranean type): high magnitude flows (3500–4500 m^3/s) in winter and spring and very low discharges (100 m^3/s on average) during the summer. Four Nuclear Power Plants (NPP), Belleville, Saint Laurent, Dampierre and Chinon, are located along the Middle Loire River and one NPP, Civaux, is located along the Vienne River. These NPP generate low-activity radioactive liquid waste, including tritium, which is released into the river in a very controlled way.

The Middle Loire River is modelled as one continuous reach with the tributaries Vienne, Indre, Cher and Maine as point inflows. Three hundreds and sixty-eight cross-sections are used to describe the river geometry. Nineteen weirs and small dams are considered. The simulated flow hydrograph covers the period 07/01/1999 to 12/31/1999 with a time step of one hour (Fig. 6). This hydrograph takes into account river-ground water exchanges as well as inflows from a number of small tributaries. The inflow discharges of the main tributaries during the same period are plotted in Fig. 6. The downstream boundary condition at MontJean is a water stage-flow rate curve. The tritium discharge recorded at Belleville NPP during the period 07/01/1999 to 12/31/1999 with a time step of one hour is specified as the upstream boundary. The tritium releases from Dampierre, Saint Laurent and Chinon NPP are introduced as lateral source terms. The tritium discharge due to release from Civaux NPP is estimated by applying *Mascaret* to the Vienne River between Civaux NPP and Vienne-Loire confluence, that is 120 km. Calibration of Strickler's coefficient is carried out using measured water levels at low, medium and high flow discharges. The Strickler coefficient is set at 30 m$^{1/3}$ s^{-1}. The time step is 10 s and the space step is 200 m, so that the CFL is smaller than 1 during the whole simulation.

Monitoring of tritium activity concentration was performed at Angers city, but the flow discharge was not measured. Although only one observation station was monitored, measurements are of great interest because they cover a long duration (*i.e.* six months). The monitoring station is 323, 287, 190, 59 and 52 km far from Belleville NPP, Dampierre NPP, Saint Laurent NPP, Chinon NPP and the lateral release from Civaux NPP, respectively. The typical mixing length L_m downstream of the lateral release from Civaux NPP (*i.e.* nearest source from the monitoring station) can be computed using the equation proposed by Chanson (2004). Because the flow is highly variable, the estimate of L_m is made for selected flow discharges, covering low, medium and high conditions. The hydraulic variables are averaged along the river

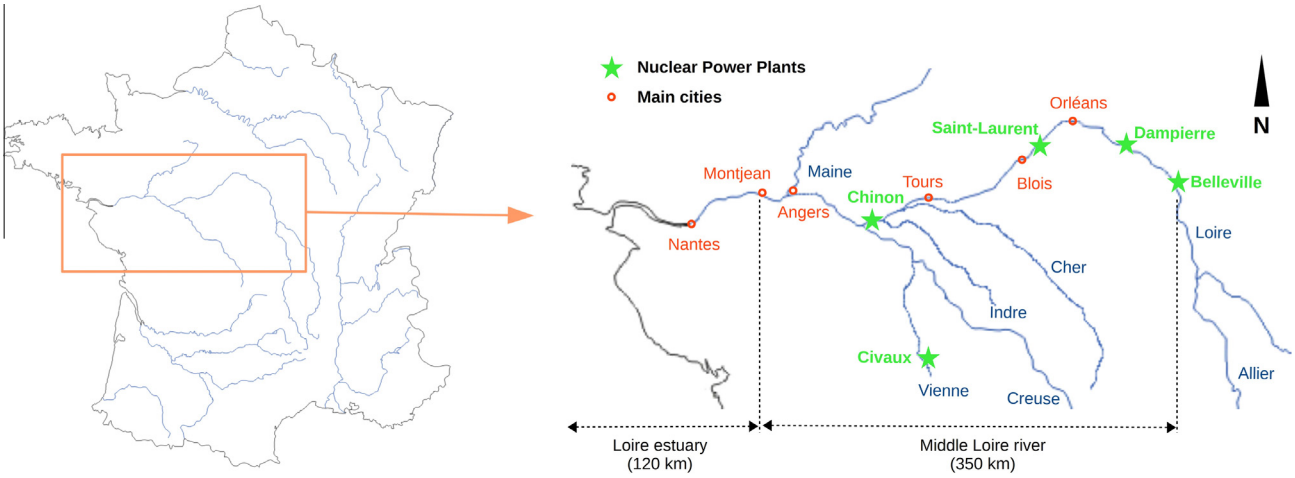

Fig. 5. Location map showing the study reach. Four main tributaries are showed. The Maine river (12 km long) is formed by the confluence of Mayenne and Sarthe.

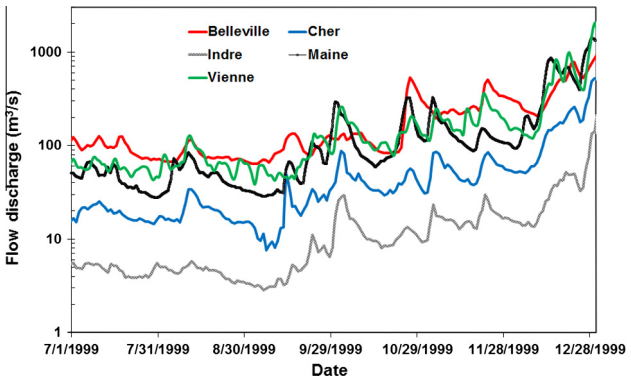

Fig. 6. Inflow hydrographs at Belleville (upstream end) and from tributaries Vienne, Indre, Cher and Maine.

reach between the Loire–Vienne confluence and Angers. The mixing length L_m is found to range between 6 km and 35 km, thus smaller than the distance separating the release location and Angers. This suggests that dispersive equilibrium should be acceptably achieved and the Fickian assumption is satisfied.

Samples were collected at the water production plant of the city which is located upstream of the Maine–Loire confluence. Water was supplied to the sampling device by a small pipe located on one of the raw water intake pipes of the plant. Automatic sampling using ISCO samples were made every 8 h (at 0:00, 08:00 and 16:00). After filtering the water sample through a 0.45 μm pore size filter, tritium concentration activity was measured by liquid scintillation counting. The average error was around 9% with a maximum value of 19%.

For the sake of brevity, we show the results obtained using the two formulas that give the best and worst results, respectively. Fig. 7 reports the comparison between the computed and measured tritium activity concentrations at Angers city. Table 5 summarises the mean relative error, ΔC, and the determination coefficient, R^2, between the computed and measured concentration curves. Comparisons between the formulations show that numerical results based on the "S&C" formula match more closely with the measurements (Fig. 7): ΔC is approximately 45% and R^2 is 0.81, indicating a remarkably good job of duplicating field data, particularly when the measurement uncertainty and the simplifications required to reduce this field case problem (where 2-or 3-D processes are locally observed) to a 1-D problem are considered. It is worth noting that the longitudinal dispersion according to "S&C" formula varies within a range of 10^{-1}–5×10^3 m^2/s.

The agreement between the observed and simulated breakthrough curves obtained with the "I&A" formula remains acceptable ($\Delta C = 48\%$ and $R^2 = 0.76$). "D" and "K&F" perform only fairly well (ΔC of 54% and 58%, respectively, and R^2 of 0.69 and 0.65, respectively). "E", L", M&K" and "M" formulas provide similar results but model-data discrepancies are high (*i.e.* ΔC is around 77% and R^2 is around 0.48). Finally, the "F" and "K&R-M" formulas display a poor performance; the relative error is particularly high ($\Delta C > 85\%$ and $R^2 < 0.42$) with activity concentrations being underestimated.

6. Discussion

6.1. General evaluation of the dispersion formulas

The longitudinal dispersion coefficient values for straight laboratory flumes may be different from that in streams, mainly because of bed geometry (*e.g.* cross-sectional shape, curvature), flow structures (*e.g.* secondary currents and recirculation zones), vegetation (Shucksmith et al., 2010), transient storage zones and macro-roughness (Parsons et al., 2007; Lane et al., 2008). Most of the empirical formulas have been calibrated and validated under specific conditions (Table 1). It is therefore not awkward that they fail in reproducing measurements in some cases. For instance, the success of "E" and "F" formulas for the small-scale experiments could be attributed to the conditions under which they were proposed and calibrated initially (*i.e.* laboratory data, uniform flow, small scale flumes, prismatic cross-sectional shape). Both formulas were found, however, not appropriate for the field case: this may be because the "E" equation ignores the transverse shear gradient, which is a main mechanism of field scale longitudinal dispersion. The "F" estimates of the dispersion coefficient are mostly overpredicted for field cases (Seo and Cheong, 1998), leading to underestimation of the concentration as was obtained for the Middle Loire River.

"Liu", "M" and "K&R-M" seem to be inappropriate for very wide streams as they did not fit data with large width-to-depth ratios (*i.e.* $B/H > 50$). This explains their poor performance in the Middle Loire River, while still performing fairly well in the laboratory cases. The "M&K" formula was proposed by relating the dispersion of a flood wave to the dispersion of solute. This analogy was highly criticized as not having an appropriate analytical basis (Fischer, 1975). The results of the present work support this limitation. The "S&C", "D" and "K&F" formulas show more success in the field case than in the laboratory cases, which is likely because these equations were a regression of a large number of field data.

Among all tested formula, only the "I&A" formula was found as being superior to existing equations in explaining dispersion characteristics in both small and large scale cases investigated in the present work. The reason is probably that this formula was calibrated over the largest set of width-to-depth ratio with B/H as small as 1 and as large as 200, and over the largest set of roughness ratio with V/V_* as small as 5 and as large as 25. Additionally, the set of data cover straight and sinuous channels (Carr, 2007), suggesting that the "I&A" formula would be suitable for both laboratory and field cases. Finally, the fit of this formula was mainly based on the parameter B/H, which is believed to be more appropriate for field cases as noted recently by Launay et al. (2015).

6.2. Sensitivity analysis

The results presented above showed that the computed concentrations depend on the formula selected for calculating the longitudinal dispersion coefficient. However, some deviations between the computed and measured concentrations still remain; the best formula does not capture the whole variability in concentrations, as one can see in the case of the Middle Loire River. This river has a complicated geometry with single and multiple channels (*i.e.* islands) and irregularly shaped cross-section. These non-uniformities of channel geometry may violate locally the main assumptions of the 1-D shallow water equations (*e.g.* presence of secondary currents, turbulence) and the advection–dispersion equation (*e.g.* transverse dispersion not negligible, well mixing of the solute over the cross-section not attained). The simulation of solute transport in this case is therefore demanding when using a 1-D numerical code, and one of the accomplished characteristics of the used model is its ability to deal with this geometry along with highly variable flow and solute discharges, while yielding concentration (using the "S&C" formula) closer to observations. If we consider the complexity that characterizes this environmental application, the level of accuracy held by the "S&C" formula ($\Delta C = 45\%$, $R^2 = 0.81$) can be considered as acceptable for a model (Kashefipour and Falconer, 2002).

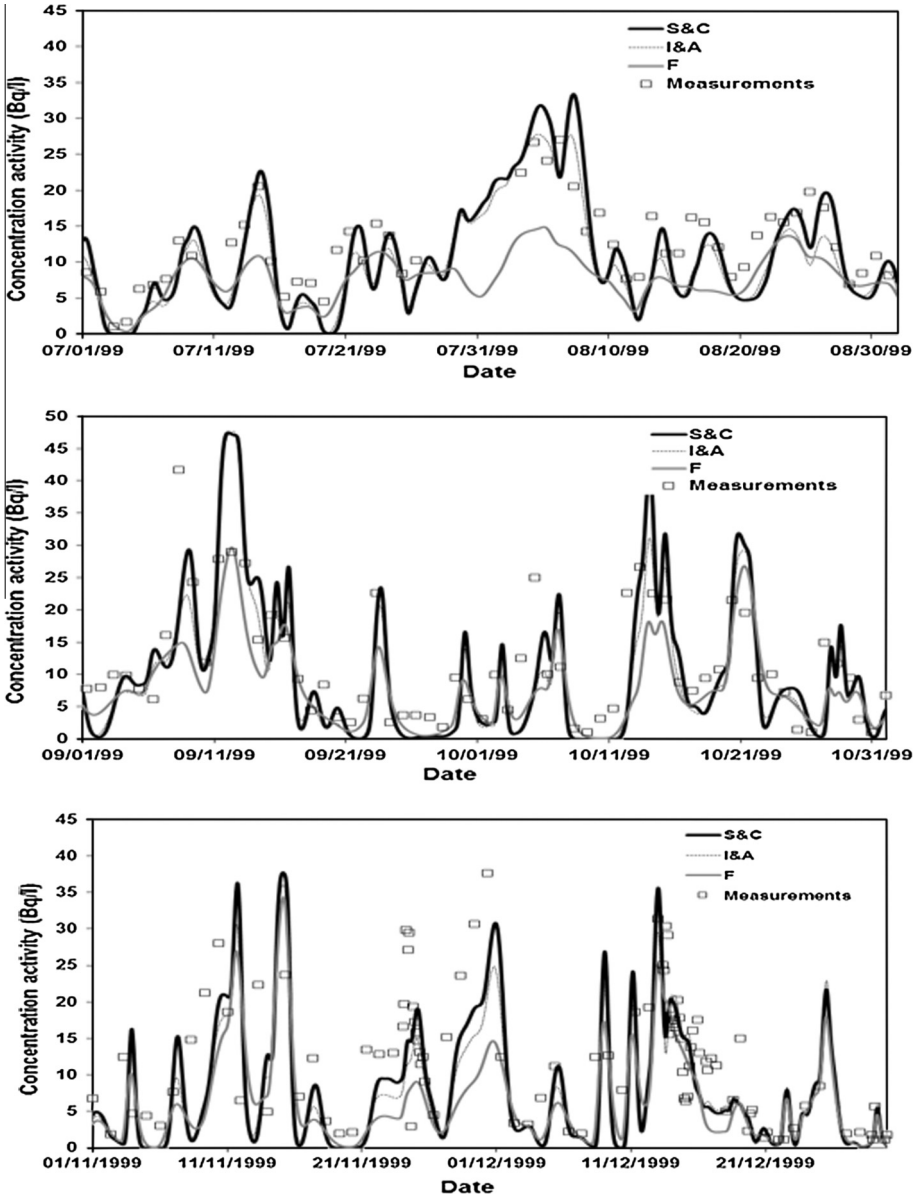

Fig. 7. Tritium activity concentration at Angers City. Comparison between numerical results and measurements.

Table 5
Middle Loire River. Accuracy of the formulas and a constant dispersion coefficient.

	E	F	M&K	L	I&A	M	K&R-M	S&C	D	K&F	D_L = 100 m^2/s
[a]ΔC (%)	75	90	80	79	48	77	87	**45**	54	58	58
[b]R^2	0.53	0.40	0.46	0.46	0.76	0.49	0.42	**0.81**	0.69	0.65	0.61

[a] Mean relative error $\Delta C[\%] = 100\sum_{i=1}^{N}|C_{c,i} - C_{m,i}|/N$.
[b] Coefficient of determination $R^2 = 1 - \sum_{i=1}^{N}(C_{c,i} - C_{m,i})^2 / \sum_{i=1}^{N} C_{m,i}^2$ (Young et al., 1980; Wilson et al., 2007). C_c and C_m are the computed and measured concentrations, respectively; N is the total number of measurements at Angers station (=229). In bold: best match between measurements and numerical results.

Hereafter, we discuss additional sources of uncertainty that may impact the numerical predictions. The Middle Loire River is selected, since this case is the most challenging one.

6.2.1. Effect of transient storage areas

The Middle Loire River involves areas of "dead zones" (or "transient storage") that take the form of pools and stagnant zone between groynes. Ignoring these areas may affect the way in which solute scatters in the river, leading to overestimation of peak concentrations and underestimation of the residence time in the stream. Dead zones can be included in the numerical modelling by modifying the advection–dispersion equation and adding an equation that describes the mass transfer between the main channel and dead zones (Deng and Jung, 2009). Solving this problem would need the knowledge of the dead zone area and residence time, which would require field tracer studies. For the Middle

Loire, there is little evidence that dead zones play a significant role. Indeed, a measure of the storage effect can be obtained by calculating the Damkohler index, *Dal*, which represents the approximate ratio of advective time of transport to dead zone residence time (Harvey et al., 1996; Schmid, 2004). The index *Dal* was calculated for various flow discharges and found in the range between 0.3 and 2.8, with the highest values being obtained at the downstream end of the river. Upstream of the monitoring station, the *Dal* is lower than 0.6, indicating that the storage areas are negligible relative to the main channel (Wagner and Harvey, 1997; Carr, 2007).

6.2.2. Effect of flow discharge estimate at Angers station

The flow discharge at Angers station was not monitored, which may have some effect on the discrepancy between measured and computed concentrations. However, calibration of the Strickler coefficient was performed using measured water levels at various low, medium and high flow discharges. This leads confidence that the computed discharge at Angers station should be accurate.

6.2.3. Effect of physical and numerical parameters

A number of physical and numerical parameters have been omitted from our analysis, which should be explored. Particularly, the computed results may depend on the space step, the time step and the Strickler coefficient. To get an insight on the effect of these parameters, additional numerical runs were performed for the different dispersion coefficient formulas. One parameter at a time was modified to determine that parameter's effect on model output. Here we present results for the "S&C" analysis; the same conclusions have been found when performing the sensitivity analysis for all other formulas.

Using a space step Δx of respectively 100 m and 400 m instead of 200 m exerts a fairly modest influence on the computed concentrations (Fig. 8); the use of Δx = 100 m does not lead to an improvement of the results. The same finding is obtained when decreasing the time step or changing the numerical scheme for the resolution of the advection equation (*i.e.* FV1 or Char. instead of FV2). Regarding the computation of the energy dissipation, we further test two values of Strickler's coefficient: 25 and 20 $m^{1/3}\,s^{-1}$. These values are selected so that measured water levels at low, medium and high flow discharges remain well reproduced by the numerical model. The overall agreement between computed and measured concentrations is slightly affected (Fig. 9); K_s = 30 $m^{1/3}\,s^{-1}$ provides the best results.

6.2.4. Empirical formula versus a constant dispersion coefficient

It is interesting to find out whether it would be sufficient to utilize only a constant longitudinal coefficient value to reproduce measurements. We performed three numerical runs using 10, 100 and 1000 m^2/s, respectively. Fig. 10 plots the computed and measured concentrations at Angers City. It is clear that

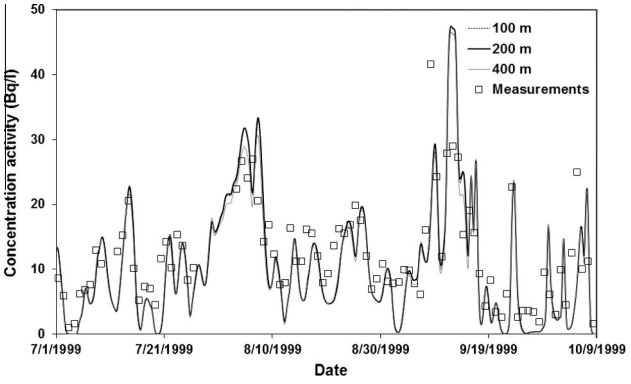

Fig. 8. Middle Loire River – Sensitivity of numerical results to changes in space step.

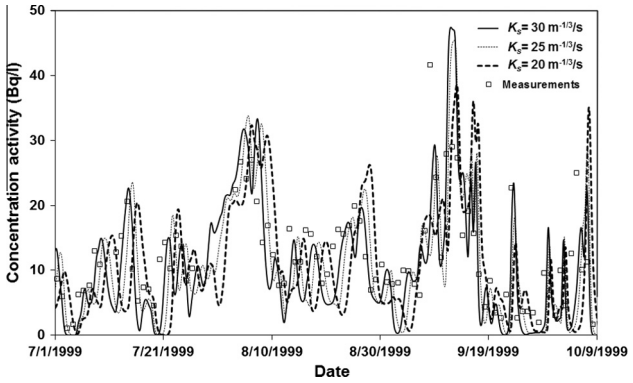

Fig. 9. Middle Loire River – Sensitivity of numerical results to changes in Strickler's coefficient value.

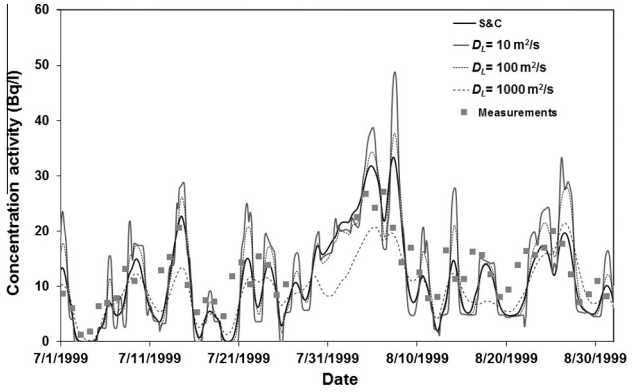

Fig. 10. Middle Loire River – "S&C" formula versus invariant dispersion coefficient.

manipulating the simulation with different values of D_L, the trend of the results change, particularly in terms of peak concentrations: deviations are typically high if a constant dispersion coefficient is used. The best results are given by D_L = 100 m^2/s, but still less accurately when compared to those of the S&C formula (Table 5). This confirms that the S&C formula adds a predictive value to the results.

7. Conclusions

The objective of this paper was to investigate the major issues associated with the calibration of longitudinal dispersion coefficient in numerical modelling of solute transport in streams. The performance of ten predictive formulas was assessed using a 1-D numerical model (open source *Mascaret* code available at www.opentelemac.org). Each formula's ability to reproduce measured breakthrough curves was tested by simulating solute transport in small and large-scale cases under steady and unsteady flow conditions. This analysis represents a new step forward assessing the applicability of dispersion coefficient formulations in numerical studies. The most important findings are:

– Simulating eight small-scale laboratory experiments (bed slope: 0.001488–0.004546, width-depth ratio: 1.5–3) of solute transport under uniform flow, results showed that for each case, concentrations are accurately reproduced using a particular formula. Based on criteria involving the peak concentration and its arrival time at various locations, Elder (1959); Fischer (1975) and Iwasa and Aya (1991) formulas ranked as the best

predictors for the entire range of conditions of the experiments. The less satisfactory results were obtained using Seo and Cheong's (1998) formula.

– In contrast, simulating the transport of tritium in the Middle Loire River (350 km long) over a long period (July 1st to December 31st 1999) with highly variable flow and complex cross-sectional geometry, Seo and Cheong's (1998) and Iwasa and Aya (1991) formulas offered the best agreement between simulated and observed concentrations, while Fischer's (1975) formula provided the less reliable results.

For the entire range of conditions studied in this work, we recommend the longitudinal dispersion coefficient formula proposed by Iwasa and Aya (1991). Evaluation of the performance of the selected formulas should be extended to other cases with complex geometry (floodplains, transient storage zones) and reactive pollutants. This is the next phase of this research and results will be reported in the future.

Acknowledgments

This work was carried out in the framework of the Project "Water Quality" funded by EDF R&D. The authors are grateful for the valuable comments of two anonymous reviewers.

References

Anderson, E.J., Phanikumar, M.S., 2011. Surface storage dynamics in large rivers: Comparing three-dimensional particle transport, one-dimensional fractional derivative, and multirate transient storage models. Water Resour. Res. 47, W09511. http://dx.doi.org/10.1029/2010WR010228.

Ani, E.C., Wallis, S., Kraslawski, A., Agachi, P.S., 2009. Development, calibration and evaluation of two mathematical models for pollutant transport in a small river. Environ. Model. Softw. 24 (10), 1139–1152.

Bencala, K.E., Walters, R.A., 1983. Simulation of solute transport in a mountain pool-and-riffle stream: a transient storage model. Water Resour. Res. 19 (3), 718–724.

Boxall, J.B., Guymer, I., 2007. Longitudinal mixing in meandering channels: new experimental data set and verification of a predictive technique. Water Res. 41 (2), 341–354.

Carr, M.L., 2007. An efficient method for measuring the dispersion coefficient in rivers. Ph.D. Dissertation, 307 p, University of Illinois, Urbana-Champaign.

Chatwin, P., 1980. Presentation of longitudinal dispersion data. J. Hydraulic Div. 106 (1), 71–83.

Chanson, H., 2004. Environmental Hydraulics of Open Channel Flows. Elsevier Butterworth-Heinemann, Burlington, MA, USA.

Chen, L., Zhu, J., Young, M.H., Susfalk, R.B., 2009. An integrated approach for modeling solute transport in streams and canals with applications. J. Hydrol. 378 (1–2), 128–136.

Cox, B.A., 2003. A review of currently available in-stream water-quality models and their applicability for simulating dissolved oxygen in lowland rivers. Sci. Total Environ. 314–316, 335–377.

Danish Hydraulic Institute (DHI), 2007. MIKE 11-A Modelling System for Rivers and Channels. Reference Manual.

De Smedt, F., 2006. Analytical solutions for transport of decaying solutes in rivers with transient storage. J. Hydrol. 330 (3–4), 672–680.

Deng, Z.Q., Jung, H.S., 2009. Scaling dispersion model for pollutant transport in rivers. Environ. Model. Softw. 24 (5), 627–631.

Deng, Z.Q., Singh, V.P., Bengtsson, L., 2001. Longitudinal dispersion coefficient in single channel streams. J. Hydraulic Eng. 128 (10), 901–916.

Elder, J.W., 1959. The dispersion of a marked fluid in turbulent shear flow. J. Fluid Mech. 5 (4), 544–560.

Etemad-Shahidi, A., Taghipour, M., 2012. Predicting longitudinal dispersion coefficient in natural streams using M5′ Model Tree. J. Hydraulic Eng. 138 (6), 542–554.

Fischer, B.H., 1975. Discussion of "Simple method for predicting dispersion in streams". J. Environ. Eng. Div. 101 (3), 453–455.

Goutal, N., 1999. The Malpasset Dam Failure-An Overview and Test Case Definition. In: Proceedings of 4th CADAM meeting, Zaragoza, 18–19 November 1999.

Goutal, N., Maurel, F., 2002. A finite volume solver for 1D shallow-water equations applied to an actual river. Int. J. Numer. Meth. Fluids 38 (1), 1–19.

Goutal, N., Luck, M., Boyer, P., Monte, L., Siclet, F., Angeli, G., 2008. Assessment, validation and inter-comparison of operational models for predicting tritium migration from routine discharges of Nuclear Power Plants: the case of Loire River. J. Environ. Radioact. 99 (2), 367–382.

Harvey, J.W., Wagner, B.J., Bencala, K.E., 1996. Evaluating the reliability of the stream tracer approach to characterize stream-subsurface water exchange. Water Resour. Res. 32 (8), 2441–2451.

Ho, D., Schlosser, P., Caplow, T., 2002. Determination of longitudinal dispersion coefficient and net advection in the tidal Hudson River with a large-scale, high resolution SF6 tracer release experiment. Environ. Sci. Technol. 36 (15), 3234–3241.

Hunt, B., 2006. Asymptotic solutions for one-dimensional dispersion in rivers. J. Hydraulic Eng. 132 (1), 87–93.

Iwasa, Y., Aya, S., 1991. Predicting longitudinal dispersion coefficient in open channel flows. In: Proceedings of International Symposium on Environmental Hydraulics, Hong Kong, pp. 505–510.

Kashefipour, M.S., Falconer, R.A., 2002. Longitudinal dispersion coefficients in natural channels. Water Res. 36 (6), 1596–1608.

Kim, D., 2012. Assessment of longitudinal dispersion coefficients using Acoustic Doppler Current Profilers in large river. J. Hydro-environment Res. 6 (1), 29–39.

Koussis, A.D., Rodriguez-Mirasol, J., 1998. Hydraulic estimation of dispersion coefficient for streams. J. Hydraulic Eng. 124 (3), 317–320.

Lane, S.N., Parsons, D.R., Best, J.L., Orfeo, O., Kostaschuk, R.A., Hardy, R.J., 2008. Causes of rapid mixing at a junction of two large rivers: Rio Parana and Rio Paraguay, Argentina. J. Geophys. Res. Earth Surf. 113 (F2). http://dx.doi.org/10.1029/2006JF000745.

Launay, M., Le Coz, J., Camenen, B., Walter, C., Angot, H., Dramaisa, G., Faure, J.-F., Coquery, M., 2015. Calibrating pollutant dispersion in 1-D hydraulic models of river networks. J. Hydro-environment Res. 9 (1), 120–132.

Leibundgut, C., Maloszewski, P., Kuülls, C., 2009. Tracers in Hydrology. Wiley-Blackwell.

Liu, H., 1977. Predicting dispersion coefficient of stream. J. Environ. Eng. Div. 103 (1), 59–69.

Magazine, M.K., Pathak, S.K., Pande, P.K., 1988. Effect of bed and side roughness on dispersion in open channels. J. Hydraulic Eng. 114 (7), 766–782.

McQuivey, R.S., Keefer, T.N., 1974. Simple method for predicting dispersion in streams. J. Environ. Eng. Div. 100 (4), 997–1011.

Parsons, D.R., Best, J.L., Lane, S.N., Orfeo, O., Hardy, R.J., Kostaschuk, R., 2007. Form roughness and the absence of secondary flow in a large confluence-diffluence, Rio Parana, Argentina, Earth Surface Processes Landforms 32(1), pp. 155–162.

Pelletier, G.J., Chapra, C.S., Tao, H., 2006. QUAL2Kw, A framework for modeling water quality in streams and rivers using a genetic algorithm for calibration. Environ. Model. Softw. 21 (3), 419–425.

Rubio, A.D., Zalts, A., El Hasi, C.D., 2008. Numerical solution of the advection–reaction–diffusion equation at different scales. Environ. Model. Softw. 23 (3), 90–95.

Runkel, R.L., 1998. One-dimensional Transport with Inflow and Storage (OTIS): a solute transport model for streams and rivers. Water Resources Investigations Report 98–4018, 80 p, United States Geological Survey.

Russell, T.F., Celia, M.A., 2002. An overview of research on Eulerian–Lagrangian Localised Adjoint Methods (ELLAM). Adv. Water Resour. 25 (8–12), 1215–1231.

Rutherford, J., 1994. River Mixing. Wiley, Chichester, UK.

Sahay, R., 2011. Prediction of longitudinal dispersion coefficients in natural rivers using artificial neural network. Environ. Fluid Mech. 11 (3), 247–261.

Schmid, B.H., 2004. Simplification in longitudinal transport modeling: case of instantaneous slug release. J. Hydrol. Eng. 9 (4), 319–324.

Seo, I.W., Baek, K.O., 2004. Estimation of the longitudinal dispersion coefficient using the velocity profile in natural streams. J. Hydraulic Eng. 130 (3), 227–236.

Seo, I.W., Cheong, T.S., 1998. Predicting longitudinal dispersion coefficient in natural Stream. J. Hydraulic Eng. 124 (1), 25–32.

Shen, C., Phanikumar, M.S., 2009. An efficient space-fractional dispersion approximation for stream solute transport modeling. Adv. Water Resour. 32 (10), 1482–1494.

Shen, C., Niu, J., Anderson, E.J., Phanikumar, M.S., 2010. Estimating longitudinal dispersion in rivers using Acoustic Doppler Current Profilers. Adv. Water Resour. 33 (6), 615–623.

Shucksmith, J.D., Boxall, J.B., Guymer, I., 2010. Effects of emergent and submerged natural vegetation on longitudinal mixing in open channel flow. Water Resour. Res. 46 (4). http://dx.doi.org/10.1029/2008WR007657.

Singh, U.P., Garde, R.J., Ranja Raju, K.G., 1992. Longitudinal dispersion in open channel flow. Int. J. Sedim. Res. 7 (3), 65–83.

Tayfur, G., Singh, V.P., 2005. Predicting longitudinal dispersion coefficient in natural streams by artificial neural network. J. Hydraulic Eng. 131 (11), 991–1000.

Toprak, Z.F., Sen, Z., Savci, S.M., 2004. Comment on "Longitudinal dispersion coefficients in natural channels". Water Res. 38 (13), 3139–3143.

UK Environment Agency, 2001. SIMCAT 7.6: A Guide and Reference for Users. UK Environment Agency, Bristol, UK.

US Army Corps of Engineers (USACE), 2010. HEC-RAS River Analysis System. User's Manual – Version 4.1. <http://www.hec.usace.army.mil/software/hec-ras/documents/HEC-RAS_4.1_Users_Manual.pdf>.

Vieira, D.A.N., 2004. Integrated Modeling of Watershed and Channel Processes. Ph.D. Dissertation, 161 p, University of Mississippi, Oxford, MS.

Wagner, B.J., Harvey, J.W., 1997. Experimental design for estimating parameters of rate-limited mass transfer: Analysis of stream tracer studies. Water Resour. Res. 33 (7), 1731–1741.

Warrick, A.W., 2003. Soil Water Dynamics. Oxford University Press, New York, 416 p.

Wilson, C.A.M.E., Guymer, I., Boxall, J.B., Olsen, N.R.B., 2007. Three-dimensional numerical simulation of solute transport in a meandering self-formed river channel. J. Hydraul. Res. 45 (5), 610–616.

Wörman, A., Packman, A.I., Johansson, H., Jonsson, K., 2002. Effect of flow-induced exchange in hyporheic zones on longitudinal transport of solutes in streams and rivers. Water Resour. Res. 38 (1). http://dx.doi.org/10.1029/2001WR000769.

Young, P., Jakeman, A., McMurtrie, R., 1980. An instrument variable method for model order identification. Automatica 16, 281–294.
Zeng, Y., Huai, W., 2014. Estimation of longitudinal dispersion coefficient in rivers. J. Hydro-environment Res. 8 (1), 2–8.
Zerihun, D., Furman, A., Warrick, A.W., Sanchez, C.A., 2005. Coupled Surface-subsurface solute transport model for irrigation Borders and Basins. I. Model Development. J. Irrig. Drain. Eng. 131 (5), 396–406.
Zhang, Y., Aral, M., 2004. Solute transport in open-channel networks in unsteady flow regime. Environ. Fluid Mech. 4 (3), 225–247.
Zhang, X.X., Qi, X.B., Zhou, X.G., 2006. An in situ method to measure the longitudinal and transverse dispersion coefficients of solute transport in soil. J. Hydrol. 328 (3–4), 614–619.
Zoppou, C., Roberts, S., Renka, R.J., 2000. Exponential spline interpolation in characteristic based scheme for solving the advective diffusion equation. Int. J. Numer. Meth. Fluids 33 (3), 129–152.
Zulfequar, A., 1997. Longitudinal dispersion of conservative pollutants in open channels. Ph.D. Dissertation, 171 p, THAPAR Institute of Engineering and Technology, India.